

# Effect of Coulomb Forces on the Position of the Pole in the Scattering Amplitude and on Its Residue

Yu. V. Orlov,<sup>1,\*</sup> B. F. Irgaziev,<sup>2,†</sup> and L. I. Nikitina<sup>1</sup>

<sup>1</sup>*Skobeltsyn Institute of Nuclear Physics, Moscow State University, Moscow, 119991 Russia*

<sup>2</sup>*Institute of Applied Physics, NUUZ, Tashkent, Uzbekistan*

(Dated: November 15, 2018)

Explicit expressions of the vertex constant for the decay of a nucleus into two charged particles for an arbitrary orbital momentum  $l$  are derived for the standard expansion of the effective-range function  $K_l(k^2)$ , as well as when the function  $K_0(k^2)$  has a pole. As physical examples, we consider the bound state of the nucleus  ${}^3\text{He}$  and the resonant states of the nuclei  ${}^2\text{He}$  and  ${}^3\text{He}$  in the  $s$ -wave, and those of  ${}^5\text{He}$  and  ${}^5\text{Li}$  in the  $p$ -wave. For the systems  $Np$  and  $Nd$  the pole trajectories are constructed in the complex planes of the momentum and of the renormalized vertex constant. They correspond to a transition from the resonance state to the virtual state while the Coulomb forces gradually decrease to zero.

PACS numbers: 21.45.+v, 24.30.Gd, 25.10.+s, 25.40.Cm, 25.40.Dn, 25.60.Bx, 25.70.Ef, 27.10.+h

## I. INTRODUCTION

The vertex constants (VC)  $G_l^2$  ( $l$  is the orbital momentum, the other quantum numbers are omitted) for  $a \leftrightarrow b + c$  virtual decay (synthesis) and the related residues of the partial elastic scattering amplitude in the pole of a bound or resonance state (when a decay is real) are considered to be independent physical quantities. They play an important role in the theory of nuclear reactions using Feynman diagrams and in astrophysics. For the first time the vertex parts of diagrams, defining an input of the specific mechanism into the cross-section of a direct nuclear reaction, were considered in the frame of the dispersion nonrelativistic approach proposed by I. S. Shapiro more than 45 years ago [1]. The main aim of this approach was giving up the perturbation theory, on which the distorted wave method is based, for processes with a strong interaction. The selection criterion for the most important diagrams is closeness to the observable physical region of the singularity of the corresponding amplitude along with the diagram “weight” produced by the product of the vertex parts. Vertex constants are directly related to the asymptotic normalization coefficient (ANC) of the wave function, determining (along with the “binding” energy) the system  $a$  at large distances between particles  $b$  and  $c$ . The Coulomb repulsion effects must be taken into account for the charged particles. In the present study the problem is solved in the frame of an effective-range theory. The preliminary results for the  $s$ -wave were published in our works [2, 3].

As far as we know, this method of finding VC has not been considered in detail in the literature with the exception of [4] where the authors attempt to find a relationship between the vertex constant  $G_l^{\text{NC}}$  (the upper indexes point to the nuclear and the Coulomb interactions) for the bound state of the nucleus  $a$  and the parameters of the standard effective-range approximation for the elastic scattering of charged particles  $b$  with  $c$  at arbitrary values of the orbital angular momentum  $l$ . Besides the binding energy  $\epsilon_{bc}$  of the nucleus  $a$  the parameter list includes the “scattering length”  $a_l$  and the “effective range”  $r_l$ . (We put these in quotes because the dimensions of  $a_l$  and  $r_l$  depend on  $l$ , the length dimension this parameters have only at  $l = 0$ ). Unfortunately, a serious error of fundamental importance was made in [4]: Eq. (25) in [4] (the numbering of the formulas in this and in the next section corresponds strictly to the numbering in [4]), which relates the binding energy to the “scattering length” and to the “effective range”, was written without allowance for the Coulomb interaction (!). Equation (25) which is inappropriate in the case of charged particles, was used there to derive a formula for the elastic-scattering amplitude {see Eq. (23) in [4]}, and the correct expression for  $\cot \delta_l^{\text{NC}}(E)$  from [5], which takes into account both the Coulomb and nuclear interactions, was substituted into it. As a result, the “hybrid” amplitude obtained thereby has neither a pole for the  $\epsilon_{bc}$  without the Coulomb interaction nor for the proper binding energy value  $\epsilon_{bc}^{\text{NC}}$  with the Coulomb interaction taken into account. Nevertheless the derivative of the numerator was taken at the binding energy  $E_{\text{cm}} = -\epsilon_{bc}$  (30) in order to obtain  $G_l^{\text{NC}}$ . Thus the expressions (30), (31) in [4] for the vertex constant of the virtual decay  $a \rightarrow b + c$  into two charged fragments are invalid. At first glance the situation can be remedied by using the experimental value of the binding energy

---

\*Electronic address: orlov@srd.sinp.msu.ru

†Present address: GIK Institute of Engineering Sciences and Technology, Topi, Pakistan

$\epsilon_{bc}$  in formula (31). But it is known that the parameters of the effective-range function change when the Coulomb interaction is taken into account. That is why one should not use formula (23) for neutral particles, which gives  $\epsilon_{bc}$  in terms of the parameters of the effective-range theory for neutral particles to find these parameters. Finding  $a_l$  and  $r_l$  by using data on the vertex constant is just one of the objectives of [4], this means using formulas (25) and (31) (or (34) for VC). Invalid formulas (25) and (34) were applied in paragraph 4.2 in [4] for the estimation of the scattering lengths and corresponding effective radii for  $\alpha t$  scattering in the  $p$ -wave by fitting the experimental ANC values for the channel spin  $S_B = 3/2$  and  $1/2$ . Because of the error mentioned above the results of this paragraph are questionable.

We derive formulas for the renormalized scattering amplitude and for the corresponding vertex constant in terms of the effective-range approximation with the Coulomb interaction taken into account. A more detailed analysis of the mistakes in [4] is given below.

The prime advantage of the approach proposed by us is the possibility of finding  $G_l^2$  using only experimental data, which allows us to obtain parameters of the effective-range function  $K_l(k^2)$ . For the arbitrary  $l$  values the standard effective-range expansion has the following form (see, for example, [5])

$$K_l(k^2) = -1/a_l + r_l k^2/2 + \dots, \quad (1)$$

where the dimensions are as follows:  $[a_l] = L^{2l+1}$ ,  $[r_l] = L^{-2l+1}$  ( $L$  is the length). The following notations are adopted:  $k = (2\mu E_{\text{cm}})^{1/2}$  is the wave number,  $\mu$  is the reduced mass,  $E_{\text{cm}}$  is the energy in the center-of-mass (cm) frame. For brevity below we omit the indexes of the energy in the cm frame  $E = E_{\text{cm}}$ . The energy in the laboratory frame we denote as  $E_{\text{lab}}$ . Here and below we use the system of units where  $\hbar=c=1$ .

For the  $Nd$  system the effective-range function has the form

$$K_0(k^2) = (-1/a_0 + C_2 k^2 + C_4 k^4)/(1 + k^2/\kappa_0^2). \quad (2)$$

The pole of the effective-range function  $K_0(k^2)$  in (2) at  $k^2 = -\kappa_0^2$ , i.e. at the energy  $E_{\text{cm}} = -E_0$ , where  $E_0 = (3/4m)\kappa_0^2$  (for the  $Nd$  system  $\mu = (2/3)m$ ,  $m$  is the nucleon mass), is a feature of the doublet  $Nd$  system [6–9]. For the  $nd$  system, the pole is at a negative energy near the threshold, i.e.  $E_0 > 0$ . For the  $pd$  system the situation is much more ambiguous. Due to the Coulomb repulsion, the measurements at very low energies are complex and unreliable. As a result the information on the scattering length and position of the pole of  $K_0(k^2)$  obtained in different works is ambiguous and contradictory. In a few analyses of the phase shift it was found that  $E_0 < 0$ . However, an analysis of the latest calculations within the three-body problem involving three-particle interaction gives  $E_0 > 0$ , with a pole located very close to the elastic scattering threshold.

In the absence of the Coulomb interaction, the effective-range function  $K_l(k^2)$  is related to the phase shift  $\delta_l(E)$  by the expression

$$K_l(k^2) = k^{2l+1} \cot \delta_l(E). \quad (3)$$

In the presence of the Coulomb repulsion, the right-hand side of the formula is transformed in the well-known way (see, for example, [10]) [42]:

$$K_l(k^2) = k^{2l+1} (c_{l\gamma})^{-1} \left[ [2\pi\gamma/(\exp(2\pi\gamma) - 1)] (\cot \delta_l^C(E) - i) + 2\gamma H(\gamma) \right], \quad (4)$$

where

$$H(\gamma) \equiv \Psi(i\gamma) + (2i\gamma)^{-1} - \ln(i\gamma), \quad (5)$$

$$(c_{l\gamma})^{-1} = \prod_{n=1}^l (1 + \gamma^2/n^2), \quad (c_{0\gamma})^{-1} = 1, \quad (6)$$

$$\delta_l^C(E) = \delta_l(E) - \sigma_l(E). \quad (7)$$

The following designations are used here:  $\delta_l(E)$  is the phase shift for the sum of the Coulomb and nuclear potentials,  $\sigma_l(E)$  is the Coulomb phase shift, determined by the relation

$$\exp(2i\sigma_l) = \Gamma(l+1+i\gamma)/\Gamma(l+1-i\gamma), \quad (8)$$

$\Psi(i\gamma)$  is the psi-function (logarithmic derivative of the gamma-function),  $\gamma = \lambda/k$  is the Sommerfeld Coulomb parameter,  $\lambda = \mu\alpha Z_b Z_c$ ,  $\alpha = e^2/\hbar c$  is the fine-structure constant; and  $Z_I$  is the charge number of the nucleus  $I$ . We also use the Bohr radius  $a_B = 1/\lambda$ . This notation was accepted in [11]. Using the explicit expression for  $\Psi(i\gamma)$  in the form of infinite sum, we can write  $H(\gamma)$  as (see, for example, [12]):

$$H(\gamma) = \frac{i\pi}{\exp(2\pi\gamma) - 1} + \gamma^2 \sum_{n=1}^{\infty} \frac{1}{n(n^2 + \gamma^2)} - \ln(\gamma) - \zeta, \quad (9)$$

where  $\zeta \approx 0.5772$  is the Euler constant.

Kok [11] was the first to show that in the presence of the Coulomb repulsion the scattering amplitude pole in the  $s$ -wave for the virtual (antibound) state shifts from the negative imaginary axis ( $\text{Im}k < 0$ ) to the fourth quadrant of the complex plane and becomes a resonance pole at  $k = k_{\text{res}} = \text{Re}k_{\text{res}} + i\text{Im}k_{\text{res}}$ . Since  $H(\gamma)$  in (9) is an explicit function of the argument  $ik$ , another pole arises at  $k = -\text{Re}k_{\text{res}} + i\text{Im}k_{\text{res}}$  in the third quadrant of the complex plane, which is symmetric relative to the imaginary axis with respect to  $k_{\text{res}}$ . For the singlet  $Np$  and the doublet  $Nd$  systems both poles are below the threshold ( $\text{Re}E_{\text{res}} < 0$ ), because  $|\text{Im}k_{\text{res}}/\text{Re}k_{\text{res}}| > 1$ . The mirror symmetry of zeros and poles with respect to the imaginary momentum axis stems from the general symmetry properties of the S-matrix (see, for example, [13, 14]).

The expression for  $\cot \delta_0^C(E)$ , valid for real positive energies  $E$  in the physical region, is given in the textbook by Landau and Lifshitz (Eq.(136.11) [15]), where an expansion of type (1) is used.

For the sake of completeness, we present the corresponding formula taken from [5], which is valid at arbitrary  $l$  value and can be used for the analytical continuation into the complex momentum plane.

$$K_l(k^2) = k^{2l+1}(c_{l\gamma})^{-1} [[2\pi\gamma/[\exp(2\pi\gamma) - 1]] \cot \delta_l^C(E) + \gamma[\Psi(1 + i\gamma) + \Psi(1 - i\gamma) - 2\ln \gamma]]. \quad (10)$$

Eq.(10) is suitable for a parametrization of the scattering phase shift. The corresponding expression for the  $p$ -wave is given in the work [16], where it was used for finding the S-matrix poles for  $N\alpha$  scattering near the elastic threshold. We recalculate these pole positions more accurately in the present work using the results of the phase shift analyses of the experimental data known from the literature. After that we calculate the renormalized VC, which were not considered in [16]. They can be used for finding the ANC of the corresponding Gamow wave functions.

In our work [2] we study the resonant subthreshold state of the nucleus  ${}^2\text{He}$  and the resonance for the  $\alpha\alpha$  system which has an extremely narrow width. The resonance positions for these states were calculated by Kok [11] using expansion (1). However, the vertex constants were not considered. The parameters for the  $pp$  scattering were borrowed from [17].

In works [2, 3] we also studied the  ${}^3\text{He}$  bound state and the subthreshold resonances in  $pd$  scattering for the most reasonable sets of constants in the expansion (2) which were fitted recently in [18, 28] using the doublet phase shift for the  $s$ -wave which was calculated for few energy values in the three-body approach [20, 21], for the  $NN$  potential AV18 and the three-particle interaction UR-IX. The necessity of using the calculation results for finding the parameters of  $K_0(k^2)$  is due to the fact that the experimental data for the  $pd$  scattering show large errors which increase while the energy decreases, and because the results of the phase shift analyses published in the literature are contradictory.

In the present work the trajectories for a transition from the resonant subthreshold state to the virtual (antibound) state for the  $Np$  and the  $Nd$  systems were constructed with a gradual decrease of the nucleon charge (the preliminary calculations were fulfilled in [3]). As a result we demonstrate the general physical nature of those corresponding states which differ only in the Coulomb interaction. A comparison of the trajectories for the different systems allows us to understand why the role of the resonance (or the virtual level) in  $Nd$  scattering is less important than in the case of  $Np$  scattering. The resonance momentum trajectory at the transition from  $pp$  to  $np$  system was previously calculated in [22] using the Eikemeier–Hakenbroich  $NN$  potential, which is independent of nucleon charge properties, and the Coulomb potential multiplied by the coefficient  $\xi$ , which changes from 0 to 1. The analytical continuation of the S-matrix onto the lower half-plane of the complex momentum was fulfilled by the Schrödinger equation solution. The resulting trajectory occurs close to the linear.

## II. METHOD FOR CALCULATING THE RENORMALIZED VERTEX CONSTANT

The scattering amplitude for charged particles can be written as the sum of the pure Coulomb amplitude  $f_{\text{Coul}}(\mathbf{k})$  and the amplitude originated from a short-range (nuclear) interaction in the presence of the Coulomb field (see, for example, [23])

$$f(\mathbf{k}) = f_{\text{Coul}}(\mathbf{k}) + f_{\text{Nucl}}(\mathbf{k}), \quad (11)$$

$$f_{\text{Coul}}(\mathbf{k}) = \sum_{l=0}^{\infty} \frac{2l+1}{2ik} (\exp(2i\sigma_l) - 1) P_l(\cos \theta), \quad (12)$$

$$f_{\text{Nucl}}(\mathbf{k}) = \sum_{l=0}^{\infty} \frac{2l+1}{2ik} \exp(2i\sigma_l) (\exp(2i\delta_l^{\text{C}}) - 1) P_l(\cos \theta). \quad (13)$$

Equation (13) is written for spinless particles. The generalization to the case of spins taken into account is elementary because the Coulomb interaction does not depend on the spin values. We consider amplitudes which are diagonal relative to spin and to orbital angular momentum values. A cross-section includes non-diagonal amplitudes as well when the spins are taken into account. In any case VC depends on one set of the quantum numbers  $l$  and  $s$ .

The Coulomb-nuclear partial scattering amplitude with the orbital angular momentum  $l$ , which has the poles we take interest in, can be written as (see (13)) [43]:

$$f_l^{\text{C}} = \exp(2i\sigma_l) f_l, \quad (14)$$

$$f_l = (\exp(2i\delta_l^{\text{C}}) - 1)/2ik = 1/(k \cot \delta_l^{\text{C}} - ik). \quad (15)$$

Let us find  $(k \cot \delta_l^{\text{C}} - ik)$  from (4) and insert the result into (14), (15). We obtain the following formulas:

$$f_l^{\text{C}} = \tilde{f}_{lN}^{\text{C}} k^{2l} \phi_l(k), \quad (16)$$

where

$$\tilde{f}_{lN}^{\text{C}} = [K_l(k^2) - 2k^{2l+1} (c_{l\gamma})^{-1} \gamma H(\gamma)]^{-1}, \quad (17)$$

$$\phi_l(k) = \exp(2i\sigma_l) [2\pi\gamma / [\exp(2\pi\gamma) - 1]] (c_{l\gamma})^{-1}. \quad (18)$$

Let us simplify the expression for  $\phi_l(k)$ . After simple transformations using the relationship (see (3.2) on page 54 in [24])

$$\Gamma(l+1+i\gamma)\Gamma(l+1-i\gamma) = \frac{\pi P_{l+1}(i\gamma)}{\gamma \text{sh}(\pi\gamma)}, \quad (19)$$

where  $P_n$  (not the Legendre polynomial) is defined by formulas

$$P_1(i\gamma) = \gamma^2, \quad P_{l+1}(i\gamma) = \gamma^2 \prod_{n=1}^l (n^2 + \gamma^2), \quad (20)$$

we receive the expression

$$\phi_l(k) = \left( \frac{\Gamma(l+1+i\gamma)}{l!} \right)^2 e^{-\pi\gamma}. \quad (21)$$

The function  $\phi_l(k)$ , which does not contain information about the nuclear interaction, coincides with the factor at the renormalized scattering amplitude given in the review [25] (see Eq.(3) in [25]).

Correspondingly, we can write the analog of the renormalized partial amplitude for a particle scattering by a short-range potential in the presence of the Coulomb interaction in terms of the effective-range function  $K_l(k^2)$  as [in the following, we use a tilde sign ( $\sim$ ) above the designation of renormalized quantities]

$$\tilde{f}_{lN}(k) = \tilde{f}_{lN}^{\text{C}} k^{2l} = \frac{k^{2l}}{[K_l(k^2) - 2\lambda k^{2l} H(\gamma) (c_{l\gamma})^{-1}]}. \quad (22)$$

According to this formula, it is obvious that the zero of the denominator in (22) when  $k = p$  is an amplitude pole.

For the standard effective-range expansion the pole position is derived from the equation (with (1) taken into account)

$$-1/a_l + r_l p^2/2 + \dots = 2\lambda p^{2l} H(\lambda/p) [(c_{l\gamma})^{-1}]|_{k=p}. \quad (23)$$

In the absence of the Coulomb interaction the pole position is defined by formula (3) at  $\cot \delta_l^C = i$  (see (15)), which leads to the following simple equation for the pole position in the effective-range approach with taking the first two terms in (1):

$$K_l(p^2) = -1/a_l + r_l p^2/2 = ip^{2l+1}. \quad (24)$$

For the bound state  $a$  of two particles when one of them is chargeless this implies the equation ( $p = i\kappa$ ,  $\kappa = \sqrt{2\mu\epsilon_{bc}} > 0$ ,  $\epsilon_{bc}$  is the binding energy)

$$1/a_l + r_l \kappa^2/2 = (-1)^l \kappa^{2l+1}, \quad (25)$$

which differs essentially from the equation (23) for charged particles.

Nevertheless, just equation (25) was used (see (25) in [4]) where in addition the factor  $(-1)^l$  was lost. Correspondingly, equation (24) in [4] is also incorrect where formula (25) was used to write the scattering amplitude. In our paper we use the right equation (23) from which the main equation of [11] was also derived for determining amplitude poles in the momentum complex plane, that is, on the nonphysical sheet of energy. The authors of [4] do not discuss the introduction of the renormalized VC which is real for a bound state (see [25]). In particular, the factor  $\exp(2i\sigma_l)$  was not included in their formula (19) for the Coulomb-nuclear amplitude. We note that it is precisely the renormalized VC is related to the ANC by the simple relationship (see [26]).

Using the VC definitions which is well known from [26] we obtain the following expression for the renormalized VC:

$$\tilde{G}_l^2 = -(\pi/\mu^2) \lim_{k \rightarrow i\kappa} (k^2 + \kappa^2) \tilde{f}_{lN}(k). \quad (26)$$

The equation (26) can be rewritten as

$$\tilde{G}_l^2 = \frac{(-2\pi/\mu^2)p^{2l+1}}{\frac{d}{dk} [K_l(k^2) - 2\lambda k^{2l} H(\gamma)(c_{l\gamma})^{-1}]_{k=p}}, \quad (27)$$

where for the standard expansion (1)  $\frac{d}{dk} [K_l(k^2)]_{k=p} = r_l p + \dots$ ,  $p = i\kappa$  is the position of the pole amplitude for a bound ( $\kappa > 0$  is real) or a resonance state ( $\text{Im} p < 0$ ,  $\text{Re} \kappa < 0$ ).

We considered in [2] both the conventional expansion of the effective-range function  $K_0(k^2)$  in powers of  $k^2$  ( $a_0$  is the scattering length,  $r_0$  is the effective radius,  $P, Q$  are the shape parameters),

$$K_0(k^2) = -1/a_0 + r_0 k^2/2 - P r_0^3 k^4 + Q r_0^5 k^6 - \dots, \quad (28)$$

which leads to

$$\tilde{G}_0^2 = \frac{2\pi\kappa/\mu^2}{\varphi(x) - [r_0\kappa + 4P(r_0\kappa)^3 + 6Q(r_0\kappa)^5 + \dots]}, \quad (29)$$

and the function with a pole (2) ( $C_0 = -1/a_0$ ), when we obtain [44]

$$\tilde{G}_0^2 = \frac{2\pi\kappa/\mu^2}{\varphi(x) - 2\kappa\kappa_0^2[-C_0 + C_2\kappa_0^2 - C_4\kappa^2(2\kappa_0^2 - \kappa^2)]/(\kappa_0^2 - \kappa^2)^2}. \quad (30)$$

The function  $\varphi(x)$  has the form ( $x = \lambda/\kappa = 1/a_B\kappa$ )

$$\varphi(x) = -1 - 2x + 2x^2\Psi'(x). \quad (31)$$

Let us remember that due to (15) the positions of the poles ( $k_{\text{res}} = i\kappa$ ) of the scattering amplitude  $f(k)$  for the bound or resonance (or virtual) states are determined by the condition

$$\cot \delta_l^C(E) = i. \quad (32)$$

### III. VERTEX CONSTANTS FOR PARTICULAR NUCLEI

The case of the  $s$ -wave ( $l = 0$ ) was considered in our papers [2, 3], where all the necessary formulas were given as well as the numerical calculation results for the nuclear systems  $NN$ ,  $Nd$  and  $\alpha\alpha$ . Several results from [2, 3] are given below for the sake of completeness. In the present paper we study more thoroughly the trajectories of the resonance momentum and the renormalized VC while the charge of the one of the particles gradually goes to zero.

#### A. The proton-proton system. The ground state of the ${}^2\text{He}$ nucleus

The results of the transcendental equation solution (23) with the parameters set, taken from [17] (without taking inaccuracy into account), found in [2], are  $k_{2\text{He}} = (0.0644 - i0.0871) \text{ fm}^{-1}$ ,  $E_{2\text{He}} = (-142 - i465) \text{ keV}$ . They differ only in the last figure from those obtained in [11]:  $k_{2\text{He}} = (0.0647 - i0.0870) \text{ fm}^{-1}$ ,  $E_{2\text{He}} = (-140 - i467) \text{ keV}$ . In [2] for the first time the renormalized vertex constant squared was also found  $\tilde{G}^2 = -(0.060 + i0.051) \text{ fm}$ . The calculation results change only weakly if the shape parameters  $P = Q = 0$ .

Let us now consider the transition from the  $pp$  system to a system without Coulomb interaction. Either  $nn$  or  $np$  system can be taken from the isotopic triplet. For the sake of certainty, we choose the singlet  $np$  system, for which (in the approximation  $P = Q = 0$ )  $a_0^{np} = (-23.719 \pm 0.013) \text{ fm}$ ,  $r_0^{np} = (2.76 \pm 0.05) \text{ fm}$  (see [17]). With this set of parameters, the virtual level energy  $E_v = -66 \text{ keV}$ .

In [2] the  $pp \rightarrow np$  transition was set by the linear relations

$$a_0(\xi) = a_0^{pp}\xi + a_0^{np}(1 - \xi); \quad (33)$$

$$r_0(\xi) = r_0^{pp}\xi + r_0^{np}(1 - \xi). \quad (34)$$

This approximation leads to a highly nonlinear trajectory of the resonance pole  $k_{\text{res}}(\xi)$  in the momentum complex plane, in contrast to the result of [22]. It is known (see, for example, [17]), that the effective radius only changes slightly when the Coulomb interaction is taken into account; therefore (34) is a good approximation. The decisive factor is the dependence of the scattering length on the product of charges, which significantly differs from the linear.

A monograph by Brown and Jackson [17] gives an approximate formula for the relation between the  $pp$  and  $np$  scattering lengths derived in accordance with the calculations performed long ago by Landau and Smorodinsky (see (4.29) and reference in [17]). In [17] it is noted, that, in spite of crude approximations, this formula with an accuracy within a few percent is valid for the potentials, which permit us to describe well the  $pp$  scattering data. Analogous formula had been derived in the work by Schwinger [27].

Introducing the coefficient  $\xi$  into this formula by the replacement  $\lambda \rightarrow \xi\lambda$ , we obtain the following relation, determining the dependence of the scattering length  $a_p(\xi)$  on  $\xi$  [2]:

$$1/a_p(\xi) = 1/a_0^{np} + 2\lambda\xi(\ln(2R\lambda\xi) + 0.33). \quad (35)$$

The value of  $R$  was not found in [17]. It was only noted that the dependence on this parameter should be weak because  $R$  is under the logarithm sign. Solving the transcendental equation (35) at  $\xi = 1$  we find  $R = 1.74 \text{ fm}$ . This value is within the margins of the radius spread for different potentials with two parameters given in [17] for the singlet  $np$  system. The dependence in the form (35) is approximated well by the relation [2]

$$1/a_p(\xi) = (1 - \xi^\beta)/a_0^{np} + \xi^\beta/a_0^{pp} \quad (36)$$

at  $\beta = 0.7$ . Clearly, nonlinear dependence  $a_p(\xi)$  is shown in Fig.1.

Finding out the dependence of the parameters of the effective-range function on  $\xi$  is a dynamic problem. Let us introduce into the Schrödinger equation an interaction  $\xi V_C(r)$ , instead of the Coulomb potential  $V_C(r)$ , where the coefficient  $\xi$  ranges within  $0 \leq \xi \leq 1$ . Thus, one must replace the Sommerfeld parameter  $\lambda \rightarrow \xi\lambda$  in all formulas. We obtain the results shown in Fig. 1 by solving the Schrödinger equation in the continuum for the  $Np$  and  $Nd$  scattering to find the energy dependence of the effective-range functions and their parameters. We use the Yukawa potential

$$V(r) = -V_0(R/r) \exp(-r/R), \quad (37)$$

as a nuclear interaction for which the parameters of the neutron-proton interaction in the singlet state are given in [17].

Let us now construct the trajectories for  $k_{\text{res}}(\xi)$  and  $\tilde{G}^2(\xi)$ . We find the parameters of the effective-range function by fitting the phase shift values calculated at low energies where the effective-range expansion is valid. The corresponding pole trajectories in the complex momentum plane are given in Fig. 2. They are close to the linear as in [22].

The calculation results show that, in accordance with the conclusion of [17], it is only the dependence of the scattering length  $a_p(\xi)$  on  $\xi$  that is important. The effective radius changes only slightly and can be described by the linear dependence (34). The corresponding curve is situated a little lower than the curve following from the Landau–Smorodinsky–Schwinger (35) (or (36) at  $\beta = 0.7$ ), because in this case the  $pp$  scattering length differs from the experimental one.

The trajectories  $\tilde{G}^2(\xi)$  in the complex plane of the renormalized vertex constant for the  $Np$  system given in Fig. 3 are also close to the linear. They are symmetric with respect to the real axis – that is, a complex conjugate. The contribution of the poles, located symmetrically with respect to the imaginary momentum axis, to the partial amplitude on the real energy axis is real in this case, as it should be for real interaction potentials.

### B. The doublet state of the $pd$ system in the $s$ -wave

With the strong correlations between the parameters  $C_2, C_4, E_0$  (2) and the scattering length  $a_0$  taken into account (see, for example, [9, 28]) it is suitable to write down the effective-range function in the form

$$K_0(k^2) = \frac{(-1 + c_2k^2 + c_4k^4)}{(a_0 + d_2k^2)} = \frac{-1 + b_1E + b_2E^2}{(a_0 + d_1E)}. \quad (38)$$

The parameters which appear in this formula have a much weaker dependence on  $a_0$ . An approximation of the results of three-body calculation of the phase shifts in the explicit form (2) and (38) can be considered as an analytical continuation of the partial scattering amplitude onto complex energy  $E$  values. This allows us to find the whole set

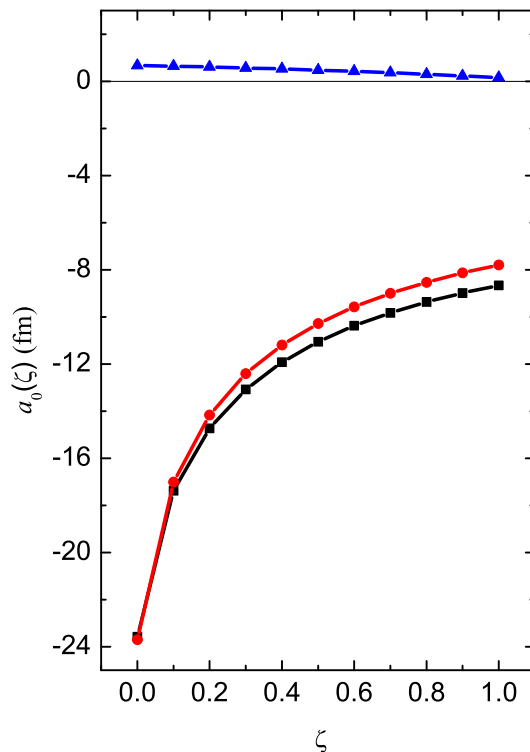


FIG. 1: The  $a_0(\xi)$  dependencies of the singlet  $Np$  scattering length (two bottom curves) and of the doublet  $Nd$  scattering length (top curve, triangles) on the coefficient  $\xi$  (multiplier before of the Coulomb potential). The results of the  $a_0(\xi)$  calculations are obtained using (35) (following the Landau–Smorodinsky–Schwinger relation between  $a_0^{pp}$  and  $a_0^{np}$ ) (circles) and by solving the Schrödinger equation with the Yukawa potential (squares).

of the low energy characteristics for the  $Nd$  system. The set includes the positions of the scattering amplitude poles for the bound and for the resonance (or virtual) state which are defined by zeroes of the denominator of (22) due to the condition (32), along with the pole position  $(-E_0)$  of the function  $K(k^2)$ .

The corresponding residues at the poles are connected with the nuclear vertex constants  $G_t^2$  and  $\tilde{G}_\tau^2$  (see [25, 26]) or with the asymptotic normalized coefficients  $C_t^2$  and  $C_\tau^2$  (see, for example, [29]) for the nuclei  ${}^3\text{H}$  and  ${}^3\text{He}$ , which for the sake of brevity are denoted by the letters  $t$  and  $\tau$  correspondingly. As is noted in the introduction, the available phase shift analyses of the experimental data for the  $pd$  scattering do not give an unambiguous result. In the first place, this affects the scattering length. Because of this, the analyses of both the modern three-body calculations with three-particle forces taken into account [20, 21, 30] and the calculation results in the frame of  $N/D$  method [31] were fulfilled in [18, 19].

Different physical observables were used for the parameter fitting: the  $s$ -wave doublet phase shift for the  $pd$  scattering at the smallest energy values considered in the literature, the binding energy of  ${}^3\text{He}$ , and the position of the subthreshold resonant pole, corresponding to the virtual state of  ${}^3\text{H}$ , which was calculated previously by the  $N/D$  method in [31], where the residue of the scattering amplitude was calculated as well. The different fitting variants were given in the tables of [18, 19].

The renormalized VC values for the selected fitting variants are given in Table 1 of our work [2] where the right  $E_{\text{res}}$  values and the parameters of the effective-range function were presented as well [45]. In the second block of this table the variants for the Argonne  $NN$  potential (AV18) with three-nucleon forces taken into account in the Urbana form (UR-IX) (see References in [20, 21]) are considered for the value  ${}^2a_{pd} = 0.024$  fm, obtained in [30] published later where the pole position of the effective-range function is also found ( $E_0 = 3.13$  MeV). This simplifies the fitting of the remaining parameters. In this case it is possible to reproduce precisely the scattering length value. Meanwhile the approximate phase shift behavior at low energy well describes the original three-body results for the interaction AV18+(UR-IX) no matter whether the binding energy is fitted or not. For this reason, we consider  ${}^2a_{pd} = 0.024$  fm as the most reliable theoretical estimation to date.

The resulting parameter value  $c_2 = {}^2a_{pd}C_2 = -58.1$  fm<sup>2</sup> found by us can be compared with the result of the analysis of the phase shift calculated in the energy region  $E_{\text{cm}} < 450$  keV by the Pisa group (see [30]) using the formula (38) when  $c_4 = 0$ . The result obtained which corresponds to the value  $c_2 = -56.7$  fm<sup>2</sup> agrees well with the results of the analysis in [19], especially for the variant No 10 ( $c_2 = -56.6$  fm<sup>2</sup>) (see Table 1 in [2]).

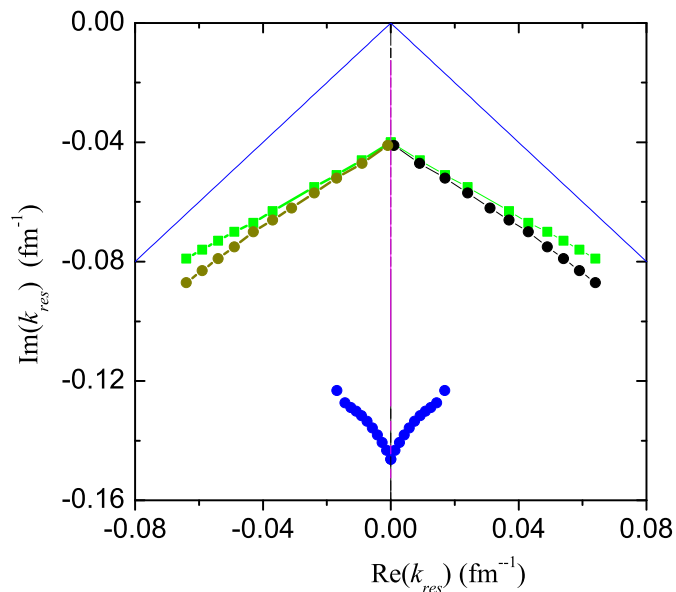


FIG. 2: Trajectories of  $k_{\text{res}}$  for the transition from the resonance pole to the virtual (antibound) state at a gradual decrease in the Coulomb interaction to zero. The top curves are trajectories for the  $Np$  system. The points correspond to different  $\xi$  values in the interval 0–1. The circles present the calculations, obtained by formula (35); the squares for the  $Np$  and points (bottom curves) for the  $Nd$  systems are obtained by solving the Schrödinger equation with the Yukawa potential. The thin straight lines are the angle bisectors of the third and fourth quadrants of the complex plane.



### 1. The bound state ${}^3\text{He}$ characteristics

The renormalized VC for the  ${}^3\text{He}$  bound state calculated in [2] in the effective-range approximation (2) occurs to be greatly underestimated (by about a factor of 2) in comparison with the results of both experimental analyses and theoretical calculations. This is due to the fact that the  ${}^3\text{He}$  bound state pole is situated far away from the convergence region for the expansion of the numerator (2) in the powers of  $k^2$ .

Unfortunately, the majority of available publications on the VC for  ${}^3\text{H}$  and  ${}^3\text{He}$  are some 20 years old. In addition, different papers report values of either the renormalized VC  $\tilde{G}^2$  or the asymptotic normalization constant (ANC)  $C^2$ . Table 1 in [2] presents both the renormalized VC and the ANC for the  ${}^3\text{He}$  bound state. The following relation between the VC and the ANC (see, for example, [28, 29]) is used:

$$\tilde{G}_\tau^2 = (27/4)\pi\kappa_\tau\lambda_N^2 C_\tau^2, \quad (39)$$

where  $\lambda_N = \hbar/mc$ ,  $\kappa_\tau$  is the wave number of the bound  ${}^3\text{He}$  nucleus. This relation corresponds to the definition of the asymptotic behavior of the normalized-to-unity relative motion wave function of the proton and the deuteron in the form (for the  $s$ -wave)

$$\psi(r) \rightarrow C_\tau N_{ZR} [W_{-\gamma, 1/2}(2\kappa_\tau r)] / r, \quad r \rightarrow \infty, \quad N_{ZR} = (2\kappa_\tau)^{1/2}, \quad (40)$$

where  $r$  is the relative distance (Jacobi coordinate) between the nucleon and the center of mass of the deuteron. This definition of the ANC corresponds to the value  $C_\tau=1$  in the zero range approximation, when the wave function coincides with its asymptotic form (40) for any ranges down to  $r=0$ .

For comparison, we give the VC and ANC data from [29], where the ANC is introduced by the relation

$$\psi(r) \rightarrow C_\tau N_W [W_{-\gamma, 1/2}(2\kappa_\tau r)] / r, \quad r \rightarrow \infty, \quad (41)$$

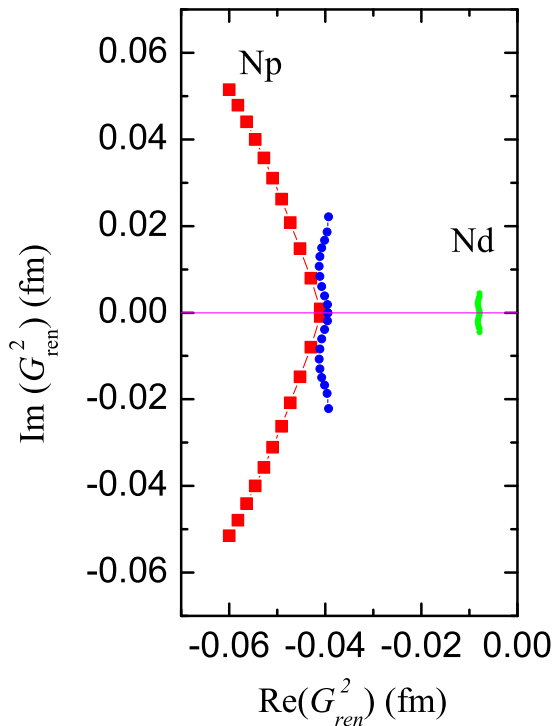


FIG. 3: Trajectories as in Fig. 2, for the square of the renormalized vertex constant,  $G_{\text{ren}}^2 \equiv (\tilde{G})^2$ , calculated with the Yukawa potential for the  $Np$  (squares) and  $Nd$  systems (on the left and right, respectively); the trajectory  $5(\tilde{G})^2$  is also shown for the  $Nd$  system.

TABLE I: The nucleon separation energies  $B_t$  and  $B_\tau$  (in MeV) for the nuclei  ${}^3\text{H}$  and  ${}^3\text{He}$ , the vertex constants  $G_t^2$  and renormalized  $\tilde{G}_\tau^2$  (in fm), the asymptotic normalized coefficients squared  $C_t^2$  and  $C_\tau^2$ , calculated in the two-body model for the different effective  $nd$  potentials (for the Hulthén potential the values are more accurate than in comparison with those given in [2]).

Potential	$B_t$	$C_t^2$	$G_t^2$	$B_\tau$	$C_\tau^2$	$\tilde{G}_\tau^2$	${}^2a_{nd}$
Hulthén	6.26	3.47	1.46	5.57	3.68	1.46	0.65
Yukawa	6.26	3.06	1.28	5.64	3.28	1.31	0.66
Tomio et al. (B)	6.26	3.56	1.49	5.60	3.77	1.50	0.65
Tomio et al. (A)	6.26	3.94	1.65	5.58	4.18	1.66	0.68

where [46]

$$(N_W)^{-2} = \int_0^\infty [W_{-\gamma,1/2}(2\kappa_\tau r)]^2 dr. \quad (42)$$

The analytical expression for  $N_W$  is given in [29], where  $N_W/N_{ZR} = 1.024$  for  ${}^3\text{He}$  (see [29]). This factor is taken into account below in the calculation of the VC from the results for  $C_\tau^2$  from (41). The calculations in [29] were carried out by solving Faddeev type equations in the configuration space for the Malfliet–Tjon (I–III) (MT) and Reid soft-core (RSC)  $NN$  potentials. The results are as follows ( $\epsilon_\tau$  is the binding energy of the  ${}^3\text{He}$  nucleus in MeV,  $\tilde{G}_\tau^2$  in fm):

$$\text{(MT)} \quad \epsilon_\tau = 7.87; \quad C_\tau^2 = 3.90; \quad \tilde{G}_\tau^2 = 1.63; \quad (43)$$

$$\text{(RSC)} \quad \epsilon_\tau = 6.39; \quad C_\tau^2 = 3.14; \quad \tilde{G}_\tau^2 = 1.12. \quad (44)$$

Coulomb effects are calculated in (43) and (44) within the point charge approximation. Allowance for spread of the charge does not affect the VC and ANC values to a precision of one-hundredth. The results for the RSC potential are considerably underestimated in comparison with those for the MT potential, first of all because the nucleus is underbound for the RSC potential. In [30] the binding energies of the  ${}^3\text{H}$  and  ${}^3\text{He}$  nuclei which are near the experimental values were found for the  $NN$  potential AV18 with the three-particle forces UR-IX taken into account. We give below the results (the units are the same as in (43) and (44)) for  ${}^3\text{H}$  and  ${}^3\text{He}$  with the interaction AV18+(UR-IX):

$$\epsilon_t = 8.49; \quad C_t^2 = 3.44; \quad G_t^2 = 1.44; \quad \epsilon_\tau = 7.75; \quad C_\tau^2 = 3.53; \quad \tilde{G}_\tau^2 = 1.39. \quad (45)$$

It has long been established in the literature that there is a correlation between the binding energy and the vertex constant (see, for example, [28] and references therein). Therefore, a good reproduction of the experimental  $\epsilon_\tau$  value is important for obtaining a reliable value of the VC. The two-body potential model [32, 33], where the binding energy and the scattering length are adjustable parameters, meets this condition.

Recently we have carried out the corresponding calculations for various potentials [34], where the potential parameters were given. The parameters of the Hulthén and Yukawa effective  $nd$  potentials were fitted to the experimental values of the  ${}^3\text{H}$  binding energy and to the doublet  $nd$  scattering length  ${}^2a_{nd}$ . On the assumption of charge independence, the same nuclear potential was used for the doublet  $pd$  system. In addition, calculations were carried out for the potentials proposed in paper by Tomio et al. [33] (versions A and B). In the case of version B, we refined the parameters beforehand to get the correct doublet  $nd$  scattering length (see reference in [34]).

The results of the calculations are presented in Table I [47]. It is noteworthy that  $G_t^2$  and  $\tilde{G}_\tau^2$  are close in value despite the noticeable difference of the ANCs. The Coulomb difference of the  ${}^3\text{He}$  and  ${}^3\text{H}$  binding energies ( $\approx 0.7$  MeV) is in rather good agreement with the experimental value  $\Delta E_c = 0.76$  MeV.

The results for  ${}^3\text{He}$  agree with the conclusion in [18, 19, 35] concerning the convergence domain of expansion (2) limited by the energies  $|E_{\text{cm}}| \leq 0.74$  MeV. This domain is determined by the position of the nearby singularity of the partial wave amplitude for the  $pd$  scattering at the energy  $E_{\text{cm}} = -\epsilon_d/3$  ( $\epsilon_d$  is the deuteron binding energy) corresponding to the Feynman diagram for the one-nucleon exchange. The poles for the bound states of the  $Nd$  system turn out to be far beyond the convergence domain. At the same time the resonance of  ${}^3\text{He}$  lies within the convergence domain as the pole for the virtual triton and therefore its position and characteristics should be less sensitive to the variant of fitting and thus more reliable. We think that the best are the fits No 7, 8 in [19].

## 2. Subthreshold resonance of the $pd$ system

Our calculation of the energy of the subthreshold resonance for the the parameter set of the effective-range function taken from [30] leads to the value  $E_{\text{res}}^{pd} = -(0.315 + i0.102)$  MeV, which differs only in the third decimal figure from the corresponding value  $E_{\text{res}}^{pd} = -(0.319 + i0.099)$  MeV for the variant No 8 in Table 1 of [2], where the binding energy of  ${}^3\text{He}$  serves as an additional fit value. Let us compare our result  $E_{\text{res}}^{pd} \approx -(0.32 + i0.10)$  MeV with other results published in the literature.

In [31] the value  $E_{\text{res}}^{pd} = -(0.432 + i0.032)$  MeV was obtained by the  $N/D$  method. The absolute value of the real part is slightly overestimated in the  $N/D$  method whereas the absolute value of the imaginary part is smaller by about a factor of three. In [22] the value  $E_{\text{res}}^{pd} = -(0.432 + i0.56)$  MeV is given, which was obtained by solving the Faddeev equation for the Eikemeier–Hackenbroich  $NN$  potential. Its real part coincides with the result of [31], but the absolute value of the imaginary part is larger than in [19] by about a factor of five and is an order of magnitude larger than in the  $N/D$  method [31], which calls for explanation. Note that the position of the virtual pole of the triton found in [22] ( $B_v = 1.62$  MeV) is also considerably larger (by a factor of more than 3) than other estimates reported in the literature.

Let us now construct the trajectories of the position of the pole and residue in it at the transition from  $pd$  to  $nd$ . As in the case of the nucleon-nucleon system, we use the Yukawa-potential model (37) with the parameters and the corresponding values of the physical quantities ANC and VC calculated by solving the Schrodinger equation for the bound and continuum states (lengths in fm, energies in MeV):

$$(\text{Yu, nd}) \quad R = 2.77, \quad V_0 = 17.46; \quad C_t^2 = 3.06, \quad \tilde{G}_t^2 = 1.28. \quad (46)$$

The parameters in (46) are fitted to the triton binding energy ( $\epsilon_t = 8.48$  MeV) and to the doublet scattering length ( ${}^2a_{nd} = 0.65$  fm) for the  $nd$  scattering in the  $s$ -wave. This model describes well the energy behavior of the phase shift for the doublet  $Nd$  scattering [34] and other low-energy characteristics which were discussed above.

We introduce the coefficient  $\xi$  into the product of charges and find the dependence of the  $s$ -wave phase shift  $\delta_0(E)$  on  $E$  in the range of the convergence of the effective-range function  $K_0^{(\xi)}(k^2)$  at different  $\xi$  values ( $0 \leq \xi \leq 1$ ).

In Fig. 4 we depict the dependencies  $K_0^{(\xi)}(E_{\text{lab}})$  on the energy in the range  $E_{\text{lab}} \leq 0.3$  MeV, where the Coulomb interaction effects are most pronounced. The calculations were performed with the set  $\xi = 0, 0.2, 0.4, 0.6, 0.8$  and  $1.0$ ; these values correspond to the downward sequence of thin curves in Fig.4 (the top and bottom curves are for  $nd$  and  $pd$  scattering, respectively). The points on the curve correspond to the phase shift values found by solving the Schrödinger equation in a continuum with the Coulomb potential  $\xi V_C(r)$ . The curves connecting the points are the results of fitting using formula (38). We took the set of fitting parameters  $c_2 = aC_2, c_4 = aC_4$  and  $E_0/a$ , which depends weakly on the scattering length  $a$ . It was found that the fitted  $aC_4$  values are unstable: they change abruptly in magnitude with a variation in  $\xi$  taking large values due to the smallness of  $k^4$  in the range of  $E$  under consideration, and even change their sign. This behavior is in agreement with the conclusion of [19] according to which the parameter  $C_4$  cannot reliably be found without fitting the binding energy of the  $Nd$  system. In the range  $E_{\text{lab}} \leq 0.3$  MeV, one can assume that  $aC_4=0$ . Such an assumption was made in [30] in determining the  $K_0(E)$  parameters for the  $pd$  system. To fit the other parameters  $a, aC_2$  and  $E_0/a$  it is sufficient to use  $K_0^{(\xi)}(E)$  at low energies in the region  $E_{\text{lab}} \leq 0.1$  MeV where the convergence of the expansion is secured. It can be seen that the found parameters for the considered set of  $\xi(E)$  make it possible to reproduce nicely the  $K_0^{(\xi)}(E)$  values calculated from the Schrödinger equation at higher energies in the range under study.

It is remarkable that the observed effect of consideration of the Coulomb interaction within the two-body model is in qualitative agreement with the results obtained within the three-body problem for the  $nd$  and  $pd$  systems. The corresponding dash-line curves are shown in Fig. 4 together with our results for  $K_0^{(\xi)}(E)$ . There is very good agreement for the  $nd$  scattering (the top curve). The significant observable differences for the  $pd$  scattering are related to the difference of the close-to-zero value  ${}^2a_{pd} = 0.024$  fm in [30] from  $0.136$  fm, the value obtained in this study within the two-body Yukawa-potential model.

The first estimate of the doublet  $pd$  scattering length within the two-body model was made in [33]; the result ( ${}^2a_{pd} \cong 0.15$  fm) is close to that obtained by us using the Yukawa potential. Let us remember that the potentials considered in [33] include three parameters fitted from the doublet  $nd$  scattering length ( ${}^2a_{nd} \cong 0.65$  fm) and the  ${}^3\text{H}$  and  ${}^3\text{He}$  binding energies.

Although there is no reliable experimental result for  ${}^2a_{pd}$  at present, we think that the three-body theoretical result in [30] is currently the best estimate.

Therefore, for the  $pd$  system one can fit the parameters of the Yukawa and Hulthén potentials by analogy with the fitting for the  $nd$  system: from the experimental binding energy ( $\epsilon_\tau = 7.73$  MeV) and the theoretical  $pd$  scattering length ( ${}^2a_{pd} = 0.024$  fm).

As a result of such fitting for the Yukawa potential we found the following parameter values and the corresponding physical quantities calculated by solving the Schrödinger equation for the bound state and continuum (lengths in fm, energies in MeV)

$$(\text{Yu, } pd) \quad R = 2.82, \quad V_0 = 16.93; \quad {}^2a_{pd} = 0.026, \quad \epsilon_\tau = 7.73, \quad C_\tau^2 = 3.30, \quad \tilde{G}_\tau^2 = 1.30. \quad (47)$$

Obviously one can ignore the difference in  ${}^2a_{pd}$  (0.024 and 0.026). The values of  $C_\tau^2$  and especially of the  $\tilde{G}_\tau^2$  in (47) differ only a little from those reported in (46) and in Table 1 for the  $nd$  system. We also calculated the features of the subthreshold  $pd$  resonance for the parameter set (47) using the effective-range function values from the Schrödinger equation by this function fitting for the set of the energy  $E_{\text{lab}}$  in the range (0.02–0.16) MeV using the formula (38). With the parameters obtained in this way and when  $b_2 = 0$  ( $b_1 = 1.216 \text{ MeV}^{-1}$ ,  $d_1 = 5.112 \text{ fm/MeV}$ ) we found  $E_{\text{res}}^{pd} = -(0.310 + i0.074) \text{ MeV}$  and  $\tilde{G}_{\text{res}}^2 = (-0.00463 \pm i0.00215) \text{ fm}$  which is in reasonable agreement with of our analysis of the three-body calculations [30] made by the Pisa group of physicists:  $E_{\text{res}}^{pd} = -(0.319 + i0.099) \text{ MeV}$ ,  $\tilde{G}_{\text{res}}^2 = (-0.00596 \pm i0.00358) \text{ fm}$ .

The differences between the corresponding parameter pairs which resulted from the breakdown of the charge independence are also small, although they lead to a rather high change of the scattering length, which is known as the value most sensitive to parameter change.

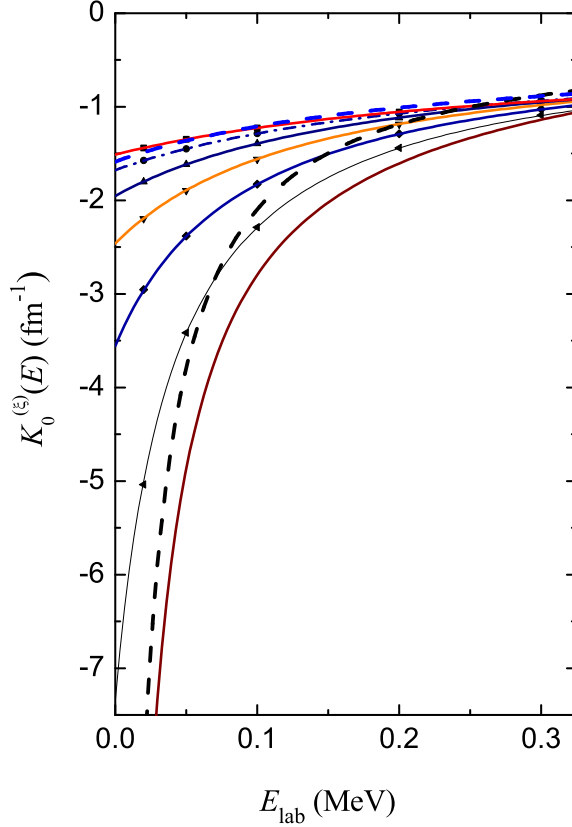


FIG. 4: The dependence of the doublet effective-range function  $K_0^{(\xi)}(E)$  on the energy  $E_{\text{lab}}$  for the  $Nd$  scattering. The sequence of the thin curves from top to bottom corresponds to the set of values  $\xi = 0, 0.2, 0.4, 0.6, 0.8$  and  $1.0$ . These calculations are fulfilled for the Yukawa-potential two-body model with the parameters (46) of the  $nd$  system using the approximation (2) when  $C_4 = 0$ . The thick dashed curves are obtained from an analysis of the three-body results [20, 21] for the Argonne  $NN$  potential (AV18) taking the three-particle Urbana forces (UR-IX) into account. The top dashed curve is for the  $nd$  scattering, the bottom dashed curve is for the  $pd$  scattering. The lowest solid thick curve shows the calculations for the Yukawa potential with the parameters (47) for the  $pd$  system.

We calculate the function  $K_0^{(\xi)}(E)$  with the parameters (47) at  $\xi = 1$  (see Fig. 4). A comparison with the three-body curve in the same figure shows that in the energy region under study the two-body model with the Yukawa potential when the parameters are fitted from the three-body binding energy value and the doublet  $pd$  scattering length given in (47) leads to a larger difference between the values of the function  $K_0^{(\xi)}(E)$  at  $\xi = 0$  and  $\xi = 1$ . This means that the role of the Coulomb repulsion is somewhat overestimated. But the observable difference between the two-body and three-body curves at  $\xi = 1$  is well known to be smaller than the experimental error. In the low-energy region considered reliable measurements of the  $pd$  scattering actually does not exist due to the high Coulomb barrier.

With the parameters of the effective-range function  $K_0^{(\xi)}(E)$  found in such a way for the Yukawa potential for the  $nd$  system we calculate  $k_{\text{res}}(\xi)$  and  $\tilde{G}^2(\xi)$ .

The charge dependence of the scattering length  ${}^2a_{Nd}(\xi)$  (the most important for the trajectory constructing) which we calculate within the two-body Yukawa-potential model with the parameters (46) is shown in Fig. 1. This function  ${}^2a_{Nd}(\xi)$  is well approximated by a quadratic polynomial

$${}^2a_{Nd}(\xi) = 0.667 - 0.273\xi - 0.244\xi^2. \quad (48)$$

The changing of the scattering length with the charge variation is quite sudden: the ratio of the scattering lengths at  $\xi = 0$  and  $\xi = 1$  is close to 4, whereas the corresponding ratio in the case of the  $Np$  scattering is near 3. The changing of the reciprocal quantity  $[{}^2a_{Nd}(\xi)]^{-1}$  is quicker. It can be described by the exponentially increasing function at  $\xi \rightarrow 1$  or as a function with a pole at  $\xi > 1$ . It should be stressed here that the relation (35) is by no means universal. Obviously, this is not valid for the system in which the effective-range function has a pole close to the scattering channel threshold. However, because of the scale difference, the changing of the  $Nd$  scattering length with the charge variation looks much weaker in Fig. 1 compared with the dependence on  $\xi$  of the  $Np$  scattering length. The corresponding curves differ not only quantitatively but also qualitatively.

The corresponding trajectories of the subthreshold resonance momentum and of the renormalized vertex constant for a transition from the spin-doublet proton-deuteron system to the neutron-deuteron system are shown in Figs. 2 and 3. Explicit qualitative and quantitative differences are seen between the corresponding trajectories for the nucleon-nucleon and nucleon-deuteron systems. In the latter case, at a transition from the resonance to the virtual state, the pole trajectory is shifted not upward but downward and is more remote from the physical energy range. The  $|\tilde{G}^2|$  magnitude for the  $Nd$  system is about factor 5 smaller than for the  $Np$  system (for clearness in Fig. 3 the trajectory ( $5\tilde{G}^2$ ) is also shown for  $Nd$  system). The charge dependence of  $\tilde{G}^2$  also differs from the case of nucleon-nucleon system.

Due to the correlation between  $E_0$  and  ${}^2a_{pd}$ , the three-body  $E_0$  value also significantly differs from the two-body model result. There is a large difference between the values of parameter  $E_0/{}^2a_{pd}$  which is less sensitive to a change in the scattering length  ${}^2a_{pd}$ . The  $E_0/{}^2a_{pd} = 0.13$  MeV/fm was obtained in the three-body approach [30] whereas the value of  $E_0/{}^2a_{pd} \approx 0.2$  MeV/fm was found in the present study on the basis of the two-body model with the Yukawa potential.

#### IV. THE $p$ -WAVE RESONANCES IN THE SCATTERING OF THE NUCLEON BY ${}^4\text{He}$

The resonances in the  $N\alpha$  scattering near the threshold have been studied in many experimental and theoretical works (see, for example, [36] and references therein). In [36] the results of the R-matrix analyses were given not only for the elastic scattering but also for the stripping and pick-up reactions. The corresponding results for the resonant energies and widths are also presented together with the experimental errors. It should be noted that the R-matrix approach used contains a considerable number of parameters. Including data on nuclear reactions in the analysis leads to additional errors due to its dependence on the model used to describe the reaction considered.

As we note in the introduction, it seems that the effective-range expansion was used for the first time in [16] to find the pole positions on the unphysical energy sheet which correspond to the resonances in the  $p$ -wave amplitude of the  $N\alpha$  elastic scattering. We limit ourselves in the present work to considering these  $p$ -wave resonances when formula (4) has the following form:

$$K_1(k^2) = k^3(1 + \gamma^2) \left[ \frac{2\pi\gamma}{\exp(2\pi\gamma) - 1} \cot \delta_l^C(E) + \gamma[\Psi(1 + i\gamma) + \Psi(1 - i\gamma) - 2 \ln \gamma] \right]. \quad (49)$$

For the renormalized VC we correspondingly derive the expression:

$$\tilde{G}_1^2 = \frac{(-2\pi/\mu^2)p^3}{\frac{d}{dk} [K_1(k^2) - (Q(k) + iC_1^2 k^3)]_{k=p}}, \quad (50)$$

TABLE II: The complex values of the resonance CM energies  $E_r - i\Gamma/2$  (in MeV) for  $j^p = 3/2^-$  and  $j^p = 1/2^-$  relative to the threshold in the channel  $\alpha + N$  ( ${}^5\text{He}$ ,  ${}^5\text{Li}$ ) and of the  $T$  matrix residues  $R_1 = |R_1|\exp(i\varphi_1)$ , ( $\varphi_1$  in deg.).

Method	Nucleus	$j^p$	$E_r$	$\Gamma$	$ R_1 $	$\varphi_1$
Eff. rad. [16]			0.778	0.639	-	-
$N/D$ [37], [25]			0.697	0.542	0.160	132
$(d, \gamma)$ [38]	${}^5\text{He}$	$3/2^-$	0.80	0.65	-	-
$R$ -function [39]			0.771	0.644	-	-
$R$ -matrix [36]			0.80	0.65	-	-
Eff. rad. (present paper);			0.778	0.641	0.171	-133
Eff. rad. [16]			1.999	4.534	-	-
$N/D$ [37], [25]			1.875	5.296	0.237	177
$R$ -function [39]	${}^5\text{He}$	$1/2^-$	1.970	5.218	-	-
$R$ -matrix [36]			2.07	5.57	-	-
Eff. rad. (present paper)			2.000	4.533	0.199	178
Eff. rad. [16]			1.637	1.292	-	-
$N/D$ [37], [25]			1.655	1.278	0.304	-136
$(d, \gamma)$ [38]	${}^5\text{Li}$	$3/2^-$	1.72	1.28	-	-
$R$ -matrix [36]			1.69	1.23	-	-
Eff. rad. (present paper);			1.630	1.437	0.278	-148
Eff. rad. [16]			2.858	6.082	-	-
$N/D$ [37], [25]	${}^5\text{Li}$	$1/2^-$	2.691	6.448	0.313	-178
$R$ -matrix [36]			3.18	6.60	-	-
Eff. rad. (present paper);			2.34	6.01	0.287	4.2

where the notations are the same as in [16]:

$$Q(k) = \gamma(1 + \gamma^2)k^3[\Psi(i\gamma) + \Psi(-i\gamma) - 2 \ln \gamma], \quad (51)$$

$$C_1^2 = 2\pi\gamma(1 + \gamma^2)/[\exp(2\pi\gamma) - 1]. \quad (52)$$

The results of our calculations are compared in Table II with those obtained in [16] and [37] (see also [25]) as well as in the more recent work [38] where the experimental data on the radiation capture of the deuteron by  ${}^3\text{H}$  and  ${}^3\text{He}$  was analyzed. As far as we know, the renormalized VCs for the resonances discussed here were previously calculated only in [37] using the  $N/D$  method and also presented in [25]. In Table II the quantity  $R_1$  for the residue of the  $T$ -matrix at the pole is given as well. It is connected with the renormalized  $\tilde{G}_l^2$  by the relationship (see [25])

$$\tilde{G}_l^2 = (-1)^l 2\pi\kappa\mu^{-2}R_l. \quad (53)$$

A comparison of our results with those presented in [25] for the  $N/D$  method shows some differences in the resonance positions and their residues. The absolute values of the residues more or less agree with each other, while the angles  $\varphi$  almost coincide in two cases but differ in the other two. The  $\varphi$  values for the states  ${}^5\text{He}$  ( $j = 1/2$ ) and  ${}^5\text{Li}$  ( $j = 3/2$ ) are in good agreement whereas for the state  ${}^5\text{He}$  ( $j = 3/2$ ) the angles  $\varphi$  differ mainly by their sign. This means that the residues are a complex conjugate. But for the state  ${}^5\text{Li}$  ( $j = 1/2$ ) the difference between them amounts to about 180 deg. This means that the residues differ approximately in their signs.

Taking the Coulomb interaction into account leads to the sign change of the angles given in [25]. In our calculations, the corresponding change of  $\varphi$  more correlates with the value of the total angular momentum  $j$  whereas the magnitude of the residue does not depend strongly on  $j$ . The inclusion of the Coulomb interaction leads to a marked increase in the absolute value  $|R_1|$  of the residue. Apparently, the noted differences between the  $\varphi$  values are not fundamental. It is known that resonance poles exist in pairs which are mirror symmetrical relative to the imaginary axis of the momentum, the corresponding residues being a complex conjugate. The sign difference of the residues also does not change the input of the poles into the cross section if there is no essential interference with a nonresonant amplitude.

In [16] the phase shift analysis of the  $N\alpha$  scattering presented in [40] was used. We compare two variants of the phase shift analysis of the  $N\alpha$  scattering which differ in their maximal energy values: (A)  $E_{\text{cm}} \leq 3$  MeV for the  $n\alpha$

scattering and  $E_{\text{cm}} \leq 5$  MeV for the  $p\alpha$  scattering [41] and (B)  $E_{\text{lab}} \leq 21$  MeV [40]. We include in Table II only our results for variant B. For the states when  $j = 1/2$  the area of the fast decrease of the phase shift is situated at a higher energy (see Fig. 5). Furthermore, the resonance width is almost ten times greater than that for the resonance when  $j = 3/2$ . At the same time, the phase shift does not pass the value  $\pi/2$ .

The short energy interval in variant A does not cover the area where the phase shift decreases quickly due to the resonance pole position. Due to this, variant A does not permit a correct reproduction of the parameters for the effective-range function. When  $j = 3/2$  the short interval is representative enough to give reasonable parameters for  $K(k^2)$  and for the corresponding resonances. The increase of the energy interval for the fitting parameters up to energy 21 MeV leads to slight differences in the results when  $j = 3/2$ . This testifies to the fact that the resonance poles considered are situated in the area where the effective-range expansion converges.

A comparison of our results with those in [16] shows excellent agreement for the  $n\alpha$  scattering but considerable disagreement for the  $p\alpha$  scattering. We believe that our calculations are more accurate due to the progress in calculation methods for equation solving, including the function  $\psi$ . In Table II the complex resonance energies calculated using the R-matrix method are generally in reasonable agreement with those obtained by other methods (see also [36]).

It should be noted that for the  $p\alpha$  scattering the agreement of our results using the analytical continuation of the effective-range function with other results published in the literature is not as good as that between the latter and the results in [16].

## V. CONCLUSIONS

Thus, in this study the correct expressions are derived for the renormalized vertex constant for the decay of a nucleus into two charged particles in a state with the arbitrary angular orbital momentum within the effective-range theory. However, it should be noted that, since this theory is valid only for low enough energies when an expansion of the effective-range function in powers of  $k^2$  converges, there is also a limitation on the upper value of the orbital angular momentum. It is likely we can largely limit ourselves to considering  $s$  and  $p$ -waves. For the  $s$ -wave ( see also [2]) we consider both the standard effective-range expansion and the expansion with a pole of the effective-range function, which is necessary in the case of the  $Nd$  system. The formulas derived are applied to the bound state of  ${}^3\text{He}$  nucleus and to the subthreshold resonance in the  $pd$  scattering which corresponds to the virtual level of  ${}^3\text{H}$  and

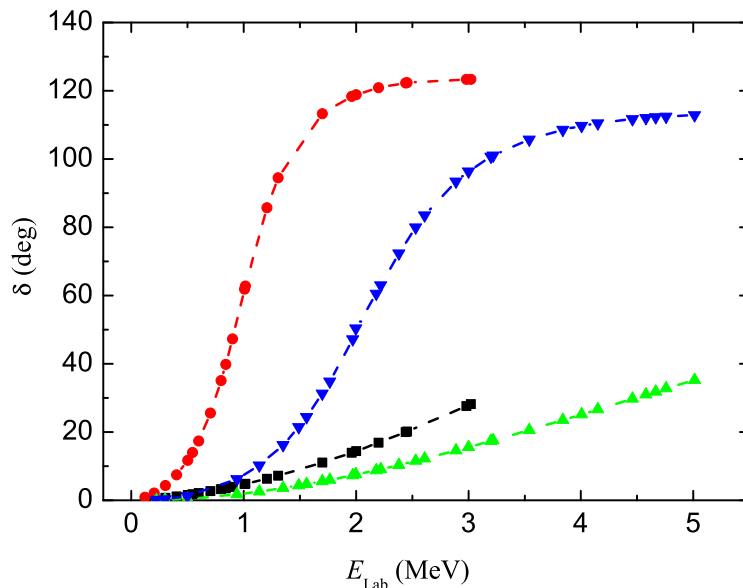


FIG. 5: The results of the phase shift analysis [41] of the nucleon scattering by the nucleus  ${}^4\text{He}$  for the  $p$ -wave: the solid circles and squares are for  $n\alpha$  scattering when  $j = 3/2$  and  $j = 1/2$  respectively, while the inverted and right triangles stand for  $p\alpha$  scattering when  $j = 3/2$  and  $j = 1/2$ , respectively.

also to the resonance of the  $pp$  system. Trajectories are constructed in the complex planes of the momentum and of the renormalized vertex constant (real for neutral particles) at the transitions from the subthreshold resonance in the ground singlet  $s$  state of the  $pp$  system to the antibound  $np$  system and from the excited doublet state of the  $pd$  system to the virtual triton state at a gradual decrease in the Coulomb interaction to zero. The constructed trajectories demonstrate the general physical nature of the corresponding states, which differ only in the Coulomb interaction.

The significant differences between the corresponding trajectories for the  $Np$  and  $Nd$  system are related to both the larger remoteness of the virtual triton pole and to the different behavior of the scattering lengths  $a(\xi)$  that depend more strongly on charge: with  $\xi$  increasing  $a(\xi)(< 0)$  quickly increases for  $Np$  scattering whereas  $a_{Nd}(\xi>(> 0))$  even more quickly decreases for  $Nd$  scattering. Because of the different scales of variation, the change for the  $Nd$  system looks slow and almost a linear decrease in Fig. 1. It is remarkable that the relatively sharp decrease in  $a_{Nd}(\xi)$  with  $\xi$  increasing due only to the Coulomb interaction, which leads to a reasonable value close to zero, was obtained by us within the simple two-body model with two parameters, fitted from the triton binding energy and doublet  $nd$  scattering length. The doublet  $pd$  scattering length found is in good agreement with the results of modern three-body calculations. The first result along these lines was obtained in [33] where the three-parameter two-body model was proposed (the third parameter was fitted from the binding energy of  ${}^3\text{He}$ ). The success of the two-body model in a qualitative reproduction of the doublet scattering length means that the internal deuteron structure is apparently of no importance at the nucleon and deuteron zero relative energy.

The parameter fitting for the Yukawa potential from the three-body  $pd$  scattering length  ${}^2a_{pd}$  considerably improves the agreement between the two-body and three-body effective-range functions at very low energies  $E_{\text{lab}} \leq 0.2$  MeV.

The reason for the difference in the trajectories for the  $Np$  and  $Nd$  systems is that a singlet deuteron is in the ground state with zero spin, for which the  $np$  interaction differs from that in the spin-triplet state, leading to the bound deuteron. The ground state of an  $Np$  system can be described within the standard effective-range approximation. The virtual triton corresponds to the excited state in which all quantum numbers, except for the principal quantum number, are the same for the real and virtual tritons. So for the virtual state one has the same effective nuclear potential as for the bound state, and the function  $K_0^{(\xi)}(k^2)$  has a pole near the threshold.

The  $|\tilde{G}^2|$  value for  $Nd$  system is smaller than for  $Np$  by a factor of about 5. Along with the larger remoteness of the pole position from the physical region, this fact explains why the  $Nd$  subthreshold poles are much more difficult to find in experiments in comparison with the well-studied  $Np$  scattering poles. The trajectory of  $k_{\text{res}}(\xi)$  which follows from the approximate formula by Landau–Smorodinsky [17] and Schwinger [27], relating  $pp$  and  $np$  scattering lengths, is in good agreement with our result for the singlet  $Np$  system in the model with the Yukawa potential. The difference is due to using the nuclear potential for the  $np$  system which leads to a small change of the  $Np$  scattering length at  $\xi = 1$  in comparison with the experimental  $pp$  scattering length.

Finally, we recalculated the resonance positions  $E_{\text{res}} - i\Gamma/2$  in the nucleon scattering on  ${}^4\text{He}$  in the  $p$ -wave within the effective-range approximation and found the corresponding residues at the poles which were then compared with the results [37,25] obtained in the  $N/D$  method.

For the  $p\alpha$  scattering when  $j = 1/2$  the  $E_{\text{res}}$  value decreased slightly and when  $j = 3/2$  the  $\Gamma$  value increased a little in comparison with the results of the work [16] where the effective-range approximation was also used.

The expressions obtained and the results of the numeral calculations of the vertex constants for nucleus decay into two charged fragments can be applied to the theory of reactions using Feynman diagrams for a description of the process mechanism, and in the analysis of astrophysical nuclear synthesis reactions.

## ACKNOWLEDGMENTS

This study was partly supported by the Russian Foundation for Basic Research, project no. 07-02-00609, and Grant NSh-485.2008.2 of the President of the Russian Federation for Support of Leading Scientific Schools.

- 
- [1] I. S. Shapiro, Zh. Eksp. Teor. Fiz. **41**, 1616 (1961) [Sov. Phys. JETP **14**, 1148 (1962)]; *Theory of Direct Nuclear Reactions* (Atomizdat, Moscow, 1963) [in Russian]; Usp. Fiz. Nauk **92**, 549 (1967) [Sov. Phys. Usp. **10**, 515 (1967)].
  - [2] V. O. Eremenko, L. I. Nikitina, and Yu. V. Orlov, Izv. Akad. Nauk, Ser. Fiz. **71**, 819 (2007) [Bull. Russ. Akad. Sci.: Physics **71**, 791 (2007)].
  - [3] Yu. V. Orlov, V. O. Eremenko, B. F. Irgaziev, and L. I. Nikitina, Izv. Akad. Nauk, Ser. fiz. **73**, 826 (2009). [Bull. Russ. Akad. Sci.: Physics **73**, 778 (2009)]
  - [4] S. B. Igamov, R. Yarmukhamedov, Nucl. Phys. A **781**, 247 (2007).



- [5] V. D. Mur, A. E. Kudryavtsev, and V. S. Popov, *Yad. Fiz.* **37**, 1417 (1983) [*Sov. J. Nucl. Phys.* **37**, 844 (1983)].
- [6] L. M. Delves, *Phys. Rev.* **118**, 1318 (1960).
- [7] W. T. H. Van Oers and J. D. Seagrave, *Phys. Lett. B* **24**, 562 (1967).
- [8] J. S. Whiting and M. G. Fuda, *Phys. Rev. C* **14**, 18 (1976).
- [9] I. V. Simenog, A. I. Sitnichenko, and D. V. Shapoval, *Yad. Fiz.* **45**, 60 (1987) [*Sov. J. Nucl. Phys.* **45**, 37 (1987)].
- [10] H. van Haeringen, *Charged-Particle Interactions (Theory and Formulas)* (Coulomb Press, Leyden, 1985).
- [11] L. P. Kok, *Phys. Rev. Lett.* **45**, 427 (1980).
- [12] J. Arvieux, *Nucl. Phys. A* **221**, 253 (1974).
- [13] A. I. Baz', Ya. B. Zel'dovich, and A. M. Perelomov, *Scattering, Reactions and Decays in Nonrelativistic Quantum Mechanics* (Nauka, Moscow, 1971) [in Russian].
- [14] A. G. Sitenko *Scattering Theory* (Vishcha Shkola, Kiev, 1975) [in Russian].
- [15] L. D. Landau and E. M. Lifshitz, *Course of Theoretical Physics, Vol. 3: Quantum Mechanics: Non-Relativistic Theory* (Nauka, Moscow, 1989; Pergamon, Oxford, 1977).
- [16] M. U. Ahmed and P. E. Shanley, *Phys. Rev. Lett.* **36**, 25 (1976).
- [17] G. E. Brown and A. D. Jackson, *Nucleon-Nucleon Interactions* (North-Holland, Amsterdam, 1976; Atomizdat, Moscow, 1979).
- [18] Yu. V. Orlov, *Izv. Akad. Nauk, Ser. Fiz.* **69**, 144 (2005) [*Bull. Russ. Akad. Sci.: Physics* **69**, 149 (2005)].
- [19] Yu. V. Orlov and Yu. P. Orevkov, *Yad. Fiz.* **69**, 855 (2006) [*Phys. At. Nucl.* **69**, 828 (2006)].
- [20] A. Kievsky, M. Viviani, and S. Rosati, *Phys. Rev. C* **52**, R15 (1995).
- [21] A. Kievsky, S. Rosati *et al.*, *Nucl. Phys. A* **607**, 402 (1996).
- [22] A. Csoto and G. M. Hale, *Phys. Rev. C* **59**, 1207 (1999); (Erratum) **62**, 049901 (2000).
- [23] M. L. Goldberger, K. M. Watson, *Collision Theory* (Wiley, New York, 1967; Mir, Moscow, 1967).
- [24] E. Janke, F. Emde, and F. Lösch, *Tables of Higher Functions* (McGrawHill, New York, 1960; Nauka, Moscow, 1964).
- [25] L. D. Blokhintsev, A. M. Mukhamedzhanov, and A. N. Safronov, *Fiz. Elem. Chastits At. Yadra* **15**, 1296 (1984) [*Sov. J. Part. Nucl.* **15**, 580 (1984)].
- [26] L. D. Blokhintsev, I. Borbely, and E. I. Dolinskii, *Fiz. Elem. Chastits At. Yadra* **8**, 1189 (1977) [*Sov. J. Part. Nucl.* **8**, 485 (1977)].
- [27] J. Schwinger, *Phys. Rev.* **78**, 135 (1950).
- [28] Yu. V. Orlov, Yu. P. Orevkov, and L. I. Nikitina, *Yad. Fiz.* **65**, 396 (2002) [*Phys. At. Nucl.* **65**, 371 (2002)].
- [29] J. L. Friar, B. F. Gibson, D. R. Lehman, and G. L. Payne, *Phys. Rev. C* **25**, 1616 (1982).
- [30] A. Kievsky, S. Rosati, M. Viviani *et al.*, *Phys. Lett. B* **406**, 292 (1997).
- [31] A. N. Safronov, *Yad. Fiz.* **50**, 951 (1989) [*Sov. J. Nucl. Phys.* **50**, 593 (1989)].
- [32] N. M. Petrov, *Yad. Fiz.* **48**, 50 (1988) [*Sov. J. Nucl. Phys.* **48**, 31 (1988)].
- [33] L. Tomio, A. Delfino, S. K. Adhikari, *Phys. Rev. C* **35**, 441 (1987).
- [34] B. F. Irgaziev, L. I. Nikitina, and Yu. V. Orlov, *Izv. Akad. Nauk, Ser. Fiz.* **70**, 227 (2006) [*Bull. Russ. Akad. Sci.: Physics* **70**, 257 (2006)].
- [35] Yu. V. Orlov and L. I. Nikitina, *Yad. Fiz.* **69**, 631 (2006) [*Phys. At. Nucl.* **69**, 607 (2006)].
- [36] A. Csoto and G. M. Hale, *Phys. Rev. C* **55**, 536 (1997).
- [37] A. N. Safronov, *Pis'ma Zh. Eksp. Teor. Fiz.* **37**, 608 (1983) [*JETP Lett.* **37**, 727 (1983)].
- [38] V. D. Efros and H. Oberhammer, *Phys. Rev. C* **54**, 1485 (1996).
- [39] J. E. Bond and F. W. K. Firk, *Nucl. Phys. A* **287**, 317 (1977).
- [40] R. A. Arndt and L. D. Roper, *Nucl. Phys. A* **209**, 447 (1973).
- [41] R. A. Arndt and L. D. Roper, *Nucl. Phys. A* **209**, 429 (1973).
- [42] A misprint in the bracket positions of this formula was made in [3] but the right formula was used for calculations.
- [43] The obviously important well known factor  $\exp(2i\sigma_l)$  written in the equation below was not included in [4].
- [44] Here, the misprint made in [2] is corrected: the factor  $\kappa_0^2$  is added in the denominator in front of the square bracket.
- [45] The accurate  $E_{\text{res}}$  results for the variants No 3, 4 are given in [19] (in [18] the values of  $k_{\text{res}}$  were given by mistake instead of  $E_{\text{res}}$  for these variants). Besides, for the case of variant No 14 in [19] the values of  $a_{pd}C_2$ ,  $a_{pd}C_4$  are wrong, they should be replaced by the values given for this variant in the table of the paper [18] (the lower line).
- [46] There is a misprint in the analogous formula (38) in [2]: the exponent of power in  $(N_W)^{-2}$  is absent.
- [47] For the Hulthén potential in Table I of the present work we give more accurate calculation results of the ANC and VC for  $^3\text{H}$  and  $^3\text{He}$ .